PHYSICAL REVIEW D **92,** 085007 (2015)

Light quarks in the screened dyon-antidyon Coulomb liquid model. II.

Yizhuang Liu,[*] Edward Shuryak,[†] and Ismail Zahed[‡]

Department of Physics and Astronomy, Stony Brook University, Stony Brook, New York 11794-3800, USA

(Received 4 May 2015; published 5 October 2015)

We discuss an extension of the dyon-antidyon liquid model that includes light quarks in the dense center symmetric phase. In this work, like in our previous one, we use the simplest color SU(2) group. We start with a single fermion flavor $N_f = 1$ and explicitly map the model onto a three-dimensional quantum effective theory with a fermion that is only $U_V(1)$ symmetric. We use it to show, in the mean-field approximation, that in the dense center, the symmetric regime leads to the nonzero chiral condensate. We estimate its value and the σ, η meson masses. We then extend our analysis to an arbitrary number of quark flavors $N_f > 1$ and colors $N_c > 2$ and show that in the dense plasma phase the spontaneous chiral symmetry breaking disappears when $N_f/N_c \geq 2$. A reorganization of the ensemble into a gas of dyon-antidyon molecules restores chiral symmetry but may still preserve center symmetry in the linearized approximation.

DOI: 10.1103/PhysRevD.92.085007 PACS numbers: 11.15.Kc, 11.30.Rd, 12.38.Lg

I. INTRODUCTION

This work is a continuation of our earlier study [1] of the gauge topology in the confining phase of a theory with the simplest gauge group $SU(2)$. We suggested that if an "instanton-dyon-antidyon" plasma is dense enough to generate strong screening, it is amenable to standard mean-field methods. Using this idea, we showed that in such a dense regime, the ensemble is indeed confining (center-symmetric).

An extensive introduction to the subject can be found in [1], so here we only mention a few basic points. The treatment of the gauge topology near and below T_c is based on the discovery of KvBLL instantons threaded by finite holonomies [2] and their splitting into the so-called instanton-dyons (antidyons), also known as instanton-monopoles or instanton-quarks. Diakonov and Petrov [3] suggested that the backreaction of the dyons on the holonomy potential at low temperature may be at the origin of the disorder-order transition of the Polyakov line. A very simple model of a deconfinement transition has been proposed by Shuryak and Sulejmanpasic [4] through the use of dyon-antidyon "repulsive cores."

The dyon-antidyon liquid model proposed by Diakonov and Petrov [3] was based on (parts of) the one-loop determinant providing the metric of the moduli spaces in BPS-protected sectors, purely self-dual or anti-self-dual. The dyon-antidyon interaction is not BPS protected and appears at the leading—classical—level, related with the so-called streamline configurations, the solutions of the "gradient flow" equation. These solutions have been recently derived by Larsen and Shuryak [5]. Their inclusion in our work [1] reveals a very strong coupling of the dyons to the antidyons, which can, however, be effectively reduced by screening, provided the dyon ensemble is dense enough.

Before turning to the main subject of this work, which is focused on the effects of light quarks on the gauge topology and chiral symmetry, we will briefly mention some important studies for the development of our work. The original discovery of the KvBLL instantons [2] with nontrivial holonomies is the key starting point for assessing the role of center symmetry on the gauge topological structures. The second important development is the assessment of the quantum weight around the KvBLL instantons in terms of the coordinates of the instanton-dyons developed by Diakonov and collaborators [3,6].

The dissociation of instantons into fractional constituents is similar to the Berezinsky-Kosterlitz-Thouless (BKT) transition in two-dimensional CPN models [7], as has been advocated by Zhitnitsky and collaborators [8], although substantially different in the details.

A center-symmetric (confining) phase can be compatible with an exponentially dilute regime that is controlled semiclassically, as shown by Unsal and Yaffe [9] using a double-trace deformation of the Yang-Mills action at large N on $S^1 \times R^3$. A similar trace deformation was used originally in the context of two-dimensional (confining) QED with unequal charges on $S^1 \times R$ [10] to analyze center symmetry and its spontaneous breaking. This construction was extended to QCD with adjoint fermions by Unsal [11] and by Unsal and others [12] to a class of deformed supersymmetric theories with soft supersymmetry breaking. While the setting includes a compactification on a small circle, with weak coupling and an exponentially *small* density of dyons, the minimum at the confining holonomy value is induced by the repulsive interaction in the dyon-antidyon pairs (called *bions* by the authors). A key role of supersymmetry is the cancellation of the

[*]yizhuang.liu@stonybrook.edu
[†]edward.shuryak@stonybrook.edu
[‡]ismail.zahed@stonybrook.edu

perturbative Gross-Pisarski-Yaffe-Weiss (GPYW) holonomy potential [13]. While this allows us to study deconfinement transition in the very dilute regime, the major subject to be studied in this work—spontaneous chiral symmetry breaking—would still be absent, as its development would require an ensemble which is sufficiently dense.

Let us now turn to the effects of light fermions. Key to these effects are topological index theorems, which relate the topological charge of the solitons to the existence and the number of its fermionic zero modes. When the ensemble of topological solitons is dense enough, the fermionic zero modes can collectivize and produce the so-called zero mode zone (ZMZ) which breaks spontaneously chiral symmetry. For the ensemble of instantons, this phenomenon has been studied in great detail in the 1980s and 1990s (for a review see [14]). Thanks to topology, the fermionic zero modes are remarkably stable against any smooth deformations of these objects, resisting a tremendous amount of perturbative noise. As has been derived in the "instanton liquid model" context and many times observed in lattice numerical simulations, the ZMZ states with Dirac eigenvalues in the range $|\lambda| \leq 20$ MeV are crucial for the generation of the hadronic masses and properties, while being only a tiny subset of all fermionic states (typically of the order of 10^{-4} in current lattice simulations).

The instanton-dyons carry fractional $1/N_c$ topological charge, while the number of the zero modes must be integers. Therefore, only some instanton-dyons may have zero modes. For physical fermions, antiperiodic on the Matsubara circle, those are L dyons (also known as KK ones). For any N_c, there is only one such dyon. Shuryak and Sulejmanpasic [15] have studied the zero modes, and the simplest effect of the fermions—binding $\bar{L}L$ dyon pairs into "molecules"—similar to instanton–anti-instanton molecules [16]. In the deformed supersymmetric setting, such molecules (called "bions" by the authors) are mostly formed due to periodic adjoint gluinos, although the effects of fundamental quarks were also addressed in [17].

Further investigations by Shuryak *et al.* [15,18] have shown that light fermions cause chiral symmetry breaking in ensembles composed of interacting dyons and antidyons, provided those are dense enough. (In the deformed supersymmetric setting, the density is exponentially small by construction, so no chiral symmetry breaking is possible.)

In this work we follow up on our study in [1], by introducing light quarks in the dense center symmetric phase of the dyon-antidyon Coulomb plasma. The word "dense" is key here, as it justifies the use of a mean-field analysis in characterizing the spontaneous breaking of chiral symmetry and the formation of a chiral condensate. As our interest is now in the light quark dynamics, we will only enforce the strong Coulomb corrections at the constraint level. One of the chief achievements of this work is to demonstrate how the induced chiral effective Lagrangian knows about confinement.

In Sec. II we detail the color SU(2) version of the model for one quark flavor $N_f = 1$. By using a series of fermionization and bosonization techniques, we show how the three-dimensional effective action for the liquid can be constructed to accommodate for the light quarks. In Sec. III we show that the ground state solution supports both center symmetry and chiral condensation. In Sec. IV we detail the flavor spectrum in terms of the sigma meson, the eta$'$ meson which is shown to be anomalous. In Sec. V we explore the effects of molecular pairing of dyons and antidyons induced by the light quarks near the transition temperature and their effect on the formation of the chiral condensate and center symmetry. In Sec. VI we briefly extend the model to include many colors and flavors and show that in the dyon-antidyon liquid with light quarks, the restoration of chiral symmetry occurs simultaneously with the loss of center symmetry for $x = N_f/N_c \geq 2$. An estimate of the transition temperature from the center symmetric to nonsymmetric phase is made. Our conclusions are in Sec. VII.

II. EFFECTIVE ACTION WITH FERMIONS

A. General setting

Since this is the second paper of the series, our notations are consistent with the first one [1] which should be consulted for details. Let us just remind the key points. In the semiclassical approximation, the Yang-Mills partition function is assumed to be dominated by an interacting ensemble of instanton-dyons (antidyons). For interparticle distances that are large compared to their sizes—or a very dilute ensemble—both the classical interactions and the one-loop effects are Coulomb-like. At distances of the order of the particle sizes, the one-loop effects are encoded in the geometry of the moduli space of the ensemble. For multidyons a plausible moduli space was argued starting from the KvBLL caloron [2] that has a number of pertinent symmetries, among which are permutation symmetry, overall charge neutrality, and clustering to KvBLL. Since the underlying calorons are self-dual, the induced metric on the moduli space was shown to be hyper-Kahler.

Specifically, and for a fixed holonomy $A_4(\infty)/2\omega_0 = \nu\tau^3/2$ with $\omega_0 = \pi T$ and $\tau^3/2$ being the only diagonal color algebra generator, the SU(2) KvBLL instanton (anti-instanton) is composed of a pair of dyons labeled by L, M (antidyons by $\bar{L}, \bar{M}$) in the notations of [3]. Generically there are $N_c - 1$ M dyons and only one twisted L dyon type. For the SU(2) gauge group used for most of our discussion, M carries (electric-magnetic) charges $(+,+)$ and L carries $(-,-)$ with fractional topological charges $v_m = \nu$ and $v_l = 1 - \nu$, respectively. Their corresponding actions are $S_L = 2\pi v_m/\alpha_s$ and $S_M = 2\pi v_l/\alpha_s$. The M dyons are also referred to as BPST dyons, while the L dyons are also called Kaluza-Klein dyons.

With the above in mind, the SU(2) grand-partition function is written as

$$\mathcal{Z}_1[T] \equiv \sum_{[K]} \prod_{i_L=1}^{K_L} \prod_{i_M=1}^{K_M} \prod_{i_{\bar{L}}=1}^{K_{\bar{L}}} \prod_{i_{\bar{M}}=1}^{K_{\bar{M}}} \int \frac{f_L d^3x_{Li_L}}{K_L!} \frac{f_M d^3x_{Mi_M}}{K_M!} \frac{f_L d^3y_{\bar{L}i_{\bar{L}}}}{K_{\bar{L}}!} \frac{f_M d^3y_{\bar{M}i_{\bar{M}}}}{K_{\bar{M}}!} \times \det(G[x]) \det(G[y]) |\det \tilde{\mathbf{T}}(x,y)| e^{-V_{D\bar{D}}(x-y)}. \quad (1)$$

Here x_{mi} and y_{nj} are the three-dimensional coordinates of the i dyon of the M kind and the j antidyon of the n kind. Here $G[x]$ is a $(K_L + K_M)^2$ matrix and $G[y]$ a $(K_{\bar{L}} + K_{\bar{M}})^2$ matrix whose explicit forms are given in [3,6]. $V_{D\bar{D}}$ is the streamline interaction between $D = L, M$ dyons and $\bar{D} = \bar{L}, \bar{M}$ antidyons as numerically discussed in [5]. For the SU(2) case its Coulomb asymptotic is [1]

$$V_{D\bar{D}}(x-y) \to -\frac{C_D}{\alpha_s T} \left(\frac{1}{|x_M - y_{\bar{M}}|} + \frac{1}{|x_L - y_{\bar{L}}|} - \frac{1}{|x_M - y_{\bar{L}}|} - \frac{1}{|x_L - y_{\bar{M}}|} \right). \quad (2)$$

The strength of the classical Coulomb interaction in (2) is $C_D/\alpha_s = 2.46/\alpha_s$. At intermediate distances $V_{D\bar{D}}$ is characterized by a core $a_{D\bar{D}} \approx 1/T$. The key new element in the partition function (1) in comparison to our previous work [1] is the introduction of the fermionic determinant $\det \tilde{\mathbf{T}}(x,y)$ that we will discuss further below.

The fugacities f_i are related to the overall dyon density. They contain the temperature-dependent running coupling constant $\alpha_s(T)$. Like [1] and earlier works, it was extracted from the temperature dependence of the fir to the measurements of the caloron plus anticaloron densities at finite temperateure in unquenched lattice simulations. We define "bare dyon density" as

$$\frac{n_D}{T^3} = C \frac{e^{-\frac{\pi}{\alpha_s(T)}}}{\alpha_s(T)^2}, \quad (3)$$

with C a constant whose value depends on the regularization scheme of the divergent determinant, and ultimately on the specific definition of $\Lambda_{\rm QCD}$. For definiteness, we will use

$$\frac{\pi}{\alpha_s(T)} = \frac{10}{3} \ln\left(\frac{T}{0.36 T_c} \right), \quad (4)$$

where $10/3 = 11N_c/6 - N_f/3$ for $N_c = 2$ and $N_f = 1$. The constant inside the logarithm has been fitted to lattice measurements of the instanton density for $N_c = 2$ and $N_f = 0$. (In principle, it should be modified along with T_c, as the theory changes, e.g. $N_f = 0$ to $N_f = 1$. Since we do not have such lattice data, we will modify only what we can, the beta function coefficient in front.)

We conclude this section by addressing some limitations of the approximations we use. While the model described by (1) can be used at any density, stability of the mean-field approximation requires that the dyonic plasma should be dense enough to produce sufficiently large screening masses (see details in [1]). In practice, this limits its application to the confined phase with $T < T_c$. The model starts to get inapplicable at high density when the dyons are close to the maximal packing density. Another limitation is that at small enough T the action per dyon $8\pi^2/g^2(T)N_c$ becomes small, thereby invalidating the use of the semiclassical approximation. Our estimates in [1] show that the model can still be used with reasonable accuracy in the range $0.5T_c < T < T_c$. Subsequent use of the mean-field analysis for the fermionic effects is aimed at the same temperature interval.

B. Quark effects

Let us start with a generic introduction. For quarks in the fundamental color representation, the squared Dirac equation in an external chromomagnetic $\mathbf{B}$ and chromoelectric $\mathbf{E}$ field takes the generic form [19] in the chiral spinor basis,

$$(-\nabla^2 + 4\mathbf{S} \cdot (\mathbf{B} \mp \mathbf{E}))\varphi^{\pm} = 0, \quad (5)$$

with $i\nabla = i\partial + A$ and $\mathbf{S}^a$ the SU(2) spin generators. The signs in (5) are locked with chirality of the quarks. In the absence of spin, there are no zero modes as $-\nabla^2$ is a semipositive operator. With spin, zero modes may occur when the spin contribution is negative in (5) and it balances the first one. For a self-dual object, $\mathbf{B} = \mathbf{E}$ and only the negative chirality quark can produce a zero mode state through the "magnetic moment term,"

$$(-\nabla^2 + 4\sigma \cdot \mathbf{B})\varphi_D^- = 0. \quad (6)$$

In the dyon the last term is $\sigma \cdot \mathbf{B} \approx \sigma \cdot \hat{r}/\rho^2$ at the core size $\rho \approx 1/\nu\omega_0$. The first term in (6) is the kinetic energy, bounded by the uncertainty principle and of order $1/\rho^2$. These two terms can indeed balance each other.

The explicit fermionic zero modes of the KvBLL instanton were discussed in [20]. It was noted that for large holonomies, when dyons are spatially separate, the zero mode is localized on one of the constituent dyons.

The zero modes of the individual SU(2) dyons were made explicit in [15]. We discuss their specific expressions in Appendix A.

The fermions can, in general, be integrated out, producing the fermionic determinant in the partition function. Its part, known in the literature as the "zero mode zone" (ZMZ), is the part of such determinants restricted to the subspace of fermionic states associated with such zero modes. The details of its usage can be found in Refs. [14].

This determinant can be viewed as a sum of closed fermionic loops with "hopping amplitudes" between dyons and antidyons. Those form the "hopping matrix" $\tilde{\mathbf{T}}$,

$$\tilde{\mathbf{T}}(x,y) \equiv \begin{pmatrix} 0 & \mathbf{T}_{ij} \\ -\mathbf{T}_{ji} & 0 \end{pmatrix}, \tag{7}$$

with dimensionality $(K_L + K_{\bar{L}})^2$. Each of the entries in $\mathbf{T}_{ij}$ is a "hopping amplitude" for a fermion between the ith L dyon and the jth $\bar{L}$ antidyon, defined via the zero mode φ_D of the dyon and the zero mode $\varphi_{\bar{D}}$ (of opposite chirality) of the antidyon.

Note that the diagonal elements of the hopping matrix are zero, by chirality, and the nondiagonal ones decrease with distance and are vanishing in an asymptotically dilute gas. So such an ensemble has a vanishing determinant and cannot exist. Depending on the dyon density and locations, the determinant can either be dominated by small (binary) loops or very long loops connecting a macroscopically large number of dyons. The first phase is called "molecular" and is dominated by dyon-antidyon clusters, reminiscent of the molecules in the instanton ensemble [16]. The second phase containing very long loops is called "collective" and leads to a nonzero quark condensate.

The hopping amplitude is the matrix element of the Dirac operator, in the background field of the dyon and antidyon. Assuming that $A_\mu \approx A_\mu^{\text{dyon}} + A_\mu^{\text{antidyon}}$ and using the Dirac equation for each zero mode, one can get rid of all gauge fields and rewrite it as a matrix element with a simple derivative only,

$$\mathbf{T}_{ij} \equiv \mathbf{T}(x_i - y_j) = \int d^4z \varphi_{\bar{D}}^\dagger(z - x_i) i(\gamma \cdot \partial) \varphi_D(z - y_j). \tag{8}$$

C. Bosonic fields

Following [1,3] the moduli determinants in (1) can be fermionized using four pairs of ghost fields $\chi^\dagger_{L,M}, \chi_{L,M}$ for the dyons and four pairs of ghost fields $\chi^\dagger_{\bar{L},\bar{M}}, \chi_{\bar{L},\bar{M}}$ for the antidyons. The ensuing Coulomb factors from the determinants are then bosonized using four boson fields $v_{L,M}, w_{L,M}$ for the dyons and similarly for the antidyons. The result is a doubling of the three-dimensional free actions obtained in [3]

$$\begin{aligned} S_{1F}[\chi, v, w] = -\frac{T}{4\pi} \int d^3x (&|\nabla \chi_L|^2 + |\nabla \chi_M|^2 + \nabla v_L \cdot \nabla w_L + \nabla v_M \cdot \nabla w_M) \\ &+ (|\nabla \chi_{\bar{L}}|^2 + |\nabla \chi_{\bar{M}}|^2 + \nabla v_{\bar{L}} \cdot \nabla w_{\bar{L}} + \nabla v_{\bar{M}} \cdot \nabla w_{\bar{M}}). \end{aligned} \tag{9}$$

For the interaction part $V_{D\bar{D}}$, we note that the pair Coulomb interaction in (1) between the dyons and antidyons can also be bosonized using standard tricks [21,22] in terms of σ and b fields. We note that σ and b are the un-Higgsed long range U(1) parts of the original magnetic field F_{ij} and electric potential A_4 (modulo the holonomy), respectively. As a result each dyon species acquire additional fugacity factors such that

$$M\colon\ e^{-b-i\sigma} \qquad L\colon\ e^{b+i\sigma} \qquad \bar{M}\colon\ e^{-b+i\sigma} \qquad \bar{L}\colon\ e^{b-i\sigma}. \tag{10}$$

Note that these assignments are consistent with those suggested in [4,12] using different arguments. As a result there is an additional contribution to the free part (9)

$$S_{2F}[\sigma, b] = \frac{T}{8} \int d^3x (\nabla b \cdot \nabla b + \nabla \sigma \cdot \nabla \sigma), \tag{11}$$

and the interaction part is now

$$\begin{aligned} S_I[v, w, b, \sigma, \chi] = -\int d^3x &e^{-b+i\sigma} f_M (4\pi v_m + |\chi_M - \chi_L|^2 + v_M - v_L) e^{w_M - w_L} \\ &+ e^{+b-i\sigma} f_L (4\pi v_l + |\chi_L - \chi_M|^2 + v_L - v_M) e^{w_L - w_M} \\ &+ e^{-b-i\sigma} f_{\bar{M}} (4\pi v_{\bar{m}} + |\chi_{\bar{M}} - \chi_{\bar{L}}|^2 + v_{\bar{M}} - v_{\bar{L}}) e^{w_{\bar{M}} - w_{\bar{L}}} \\ &+ e^{+b+i\sigma} f_{\bar{L}} (4\pi v_{\bar{l}} + |\chi_{\bar{L}} - \chi_{\bar{M}}|^2 + v_{\bar{L}} - v_{\bar{M}}) e^{w_{\bar{L}} - w_{\bar{M}}} \end{aligned} \tag{12}$$

without the fermions. We now show the minimal modifications to (12) when the fermionic determinantal interaction is present.

D. Fermionic fields

The determinant for the hopping fermionic zero mode can be fermionized using standard methods. For that, each entry $\mathbf{T}(x-y)$ in (1) can be viewed as a cross two-body dyon-antidyon hopping matrix with a two-body inverse $\mathbf{TG}=\mathbf{1}$. To fermionize the determinant, we define the additional Grassmanians $\chi=(\chi_1^i,\chi_2^j)^T$ with $i,j=1,\ldots,K_{L,\bar{L}}$ and

$$|\det\tilde{\mathbf{T}}|=\int D[\chi]e^{\chi^\dagger\tilde{\mathbf{T}}\chi}. \tag{13}$$

We can rearrange the exponent in (13) by defining a Grassmanian source $J(x)=(J_1(x),J_2(x))^T$ with

$$J_1(x)=\sum_{i=1}^{K_L}\chi_1^i\delta^3(x-x_{Li})$$
$$J_2(x)=\sum_{j=1}^{K_{\bar{L}}}\chi_2^j\delta^3(x-y_{\bar{L}j}) \tag{14}$$

and by introducing two additional fermionic fields $\psi(x)=(\psi_1(x),\psi_2(x))^T$. Thus,

$$e^{\chi^\dagger\tilde{\mathbf{T}}\chi}=\frac{\int D[\psi]\exp(-\int\psi^\dagger\tilde{\mathbf{G}}\psi+\int J^\dagger\psi+\int\psi^\dagger J)}{\int dD[\psi]\exp(-\int\psi^\dagger\tilde{\mathbf{G}}\psi)} \tag{15}$$

with $\tilde{\mathbf{G}}$ a 2×2 chiral block matrix,

$$\tilde{\mathbf{G}}=\begin{pmatrix}0 & \mathbf{G}(x,y)\\ -\mathbf{G}(x,y) & 0\end{pmatrix}, \tag{16}$$

with entries $\mathbf{TG}=\mathbf{1}$. The Grassmanian source contributions in (15) generate a string of independent exponents for the L dyons and $\bar{L}$ antidyons:

$$\prod_{i=1}^{K_L}e^{\chi_1^{i\dagger}\psi_1(x_{Li})+\psi_1^\dagger(x_{Li})\chi_1^i}\times\prod_{j=1}^{K_{\bar{L}}}e^{\chi_2^{j\dagger}\psi_2(y_{\bar{L}j})+\psi_2^\dagger(y_{\bar{L}j})\chi_2^j}. \tag{17}$$

The Grassmanian integration over the χ_i in each factor in (17) is now readily done to yield

$$\prod_i[-\psi_1^\dagger\psi_1(x_{Li})]\prod_j[-\psi_2^\dagger\psi_2(y_{\bar{L}j})] \tag{18}$$

for the L dyons and $\bar{L}$ antidyons. The net effect of the additional fermionic determinant in (1) is to shift the L-dyon and $\bar{L}$-antidyon fugacities in (12) through

$$f_L\to-f_L\psi_1^\dagger\psi_1\equiv-f_L\psi^\dagger\gamma_+\psi$$
$$f_{\bar{L}}\to-f_{\bar{L}}\psi_2^\dagger\psi_2\equiv-f_{\bar{L}}\psi^\dagger\gamma_-\psi, \tag{19}$$

where we have now identified the chiralities through $\gamma_\pm=(1\pm\gamma_5)/2$. The fugacities $f_{M,\bar{M}}$ are left unchanged since they do not develop zero modes.

E. Resolving the constraints

In terms of (9)–(12) and the substitution (19), the dyon-antidyon partition function (1) for $N_f=1$ can be exactly rewritten as an interacting effective field theory in three dimensions,

$$\mathcal{Z}_1[T]\equiv\int D[\psi]D[\chi]D[v]D[w]D[\sigma]D[b]\times e^{-S_{1F}-S_{2F}-S_I-S_\psi}, \tag{20}$$

with the additional $N_f=1$ chiral fermionic contribution $S_\psi=\psi^\dagger\tilde{\mathbf{G}}\psi$. In the presence of the fermionic fields ψ and the screening fields σ,b, the three-dimensional effective field theory (20) is not integrable. Simple approximation schemes will be developed to address this effective action.

Note that the effective action in (20) is linear in the $v_{M,L,\bar{M},\bar{L}}$. These are auxiliary fields that integrate into delta-function constraints. However, and for convenience, it is best to shift away the b,σ fields from (12) through

$$w_M-b+i\sigma\to w_M$$
$$w_{\bar{M}}-b-i\sigma\to w_{\bar{M}}, \tag{21}$$

which carries a unit Jacobian and no anomalies, and recover them in the pertinent arguments of the delta function constraints as

$$-\frac{T}{4\pi}\nabla^2w_M+f_Me^{w_M-w_L}-f_L\psi^\dagger\gamma_+\psi e^{w_L-w_M}=\frac{T}{4\pi}\nabla^2(b-i\sigma)$$
$$-\frac{T}{4\pi}\nabla^2w_L-f_Me^{w_M-w_L}+f_L\psi^\dagger\gamma_+\psi e^{w_L-w_M}=0, \tag{22}$$

and similarly for the antidyons. To proceed further, the formal classical solutions to the constraint equations or $w_{M,L}[\sigma,b]$ should be inserted back into the three-dimensional effective action. As in [3] we observe that the classical solutions to (22) can be used to integrate the w's in (20) to one loop. The resulting bosonic determinant cancels against the fermionic determinant after also integrating over the χ's in (20). The result is

$$\mathcal{Z}_1[T] = \int D[\psi]D[\sigma]D[b]e^{-S}, \tag{23}$$

with the three-dimensional effective action

$$\begin{aligned} S = S_F[\sigma, b] &+ \int d^3x \psi^\dagger \tilde{\mathbf{G}} \psi \\ &- 4\pi f_M v_m \int d^3x (e^{w_M - w_L} + e^{w_{\bar{M}} - w_{\bar{L}}}) \\ &+ 4\pi f_L v_l \int d^3x \psi^\dagger \gamma_+ \psi e^{w_L - w_M} \\ &+ 4\pi f_{\bar{L}} v_l \int d^3x \psi^\dagger \gamma_- \psi e^{w_{\bar{L}} - w_{\bar{M}}}. \end{aligned} \tag{24}$$

Here S_F is S_{2F} in (11) plus additional contributions resulting from the $w_{M,L}(\sigma, b)$ solutions to the constraint equations (22) after their insertion back. This procedure for the linearized approximation of the constraint was discussed in [1] for the case without fermions.

III. SU(2) QCD WITH ONE QUARK FLAVOR

To analyze the ground state and the fermionic fluctuations we bosonize the fermions in (23) by introducing two delta functions and reexponentiating them,

$$\begin{aligned} \mathcal{Z}_1[T] = \int D[\psi]D[\sigma]D[b]D[\Sigma]D[\Sigma_5]D[\lambda]D[\lambda_5] \\ \times e^{-S + \int d^3x i\lambda(\psi^\dagger\psi + \Sigma) + \int d^3x i\lambda_5(\psi^\dagger i\gamma_5 \psi + \Sigma_5)}. \end{aligned} \tag{25}$$

The ground state is parity even so that $f_{L,M} = f_{\bar{L},\bar{M}}$ and $\Sigma_5 = 0$. By translational invariance, the SU(2) ground state corresponds to constant σ, b, Σ. The classical solutions to the constraint equations (22) are also constant,

$$(e^{w_M - w_L})_0 = \sqrt{f_L \Sigma / 2 f_M}, \tag{26}$$

and similarly for the antidyons.

A. Effective potential

The effective potential $\mathcal{V}$ for constant fields follows from (25) by enforcing the delta-function constraint (25) and parity,

$$\begin{aligned} -\mathcal{V}/\mathbb{V}_3 = &+ i\lambda\Sigma + 4\pi f_M v_m (e^{w_M - w_L} + e^{w_{\bar{M}} - w_{\bar{L}}}) \\ &+ 2\pi f_L v_l \Sigma (e^{w_L - w_M} + e^{w_{\bar{L}} - w_{\bar{M}}}), \end{aligned} \tag{27}$$

with $\mathbb{V}_3$ the 3-volume. For fixed holonomies $v_{m,l}$, the constant w' s are real by (22) as all right-hand sides vanish, and the extrema of (27) occur for

$$\begin{aligned} e^{w_M - w_L} &= \pm\sqrt{\Sigma f_L v_l / 2 f_M v_m} \\ e^{w_{\bar{M}} - w_{\bar{L}}} &= \pm\sqrt{\Sigma f_L v_{\bar{l}} / 2 f_M v_{\bar{m}}}, \end{aligned} \tag{28}$$

and Eqs. (28) are consistent with (26) only if $v_l = v_m = 1/2$ and $v_{\bar{l}} = v_{\bar{m}} = -1/2$, that is, for confining holonomies or a center symmetric ground state. Thus,

$$-\mathcal{V}/\mathbb{V}_3 = i\lambda\Sigma + 8\pi\sqrt{f_L f_M \Sigma/2}. \tag{29}$$

We note that for $\Sigma = 0$ there are no solutions to the extrema equations. The holonomies are no longer constrained to the center symmetric state. Since $\Sigma = 0$ means a zero chiral condensate (see below), we conclude that in this model of the dyon-antidyon liquid with light quarks, chiral symmetry restoration and the loss of center symmetry occur simultaneously.

For the vacuum solution, the auxiliary field λ is also a constant. The fermionic fields in (25) can be integrated out. The result is a new contribution to the potential (29):

$$\begin{aligned} -\mathcal{V}/\mathbb{V}_3 \to &+ i\lambda\Sigma + 8\pi\sqrt{f_L f_M \Sigma/2} \\ &+ \int \frac{d^3p}{(2\pi)^3} \ln(1 - \lambda^2 \mathbf{T}^2(p)). \end{aligned} \tag{30}$$

The saddle point of (30) in Σ is the solution to

$$i\lambda + \frac{\alpha}{\sqrt{\Sigma}} = 0 \to \lambda = \frac{\alpha}{\sqrt{\Sigma}} \tag{31}$$

after the substitution $\lambda \to i\lambda$ with $\alpha = 4\pi\sqrt{f_L f_M/2}$. Inserting (31) into the effective potential (30) yields

$$-\mathcal{V}/\mathbb{V}_3 = \frac{\alpha^2}{\lambda} + \int \frac{d^3p}{(2\pi)^3} \ln(1 + \lambda^2 \mathbf{T}^2(p)). \tag{32}$$

The saddle point for λ is

$$\frac{\alpha^2}{2\lambda} = \int \frac{d^3p}{(2\pi)^3} \frac{\lambda^2 \mathbf{T}^2(p)}{1 + \lambda^2 \mathbf{T}^2(p)} \equiv V_0. \tag{33}$$

It is readily checked that (33) enforces the true minimum condition $d(\mathcal{V}/\mathbb{V}_3) = 0$. From (A3) we note that $\lambda\mathbf{T}(p) \approx \lambda\omega_0^4/p^6$ falls rapidly with momentum for $p > p_{\max}$ with $p_{\max}^3 \equiv \omega_0^2\sqrt{\lambda}$. A simple solution to (33) follows from the condition $\lambda\mathbf{T}(0) \gg 1$, i.e.,

$$V_0 \approx p_{\max}^3 \equiv \omega_0^2\sqrt{\lambda}. \tag{34}$$

The precise value of V_0 is not important as it will be traded for the dyon density below. Note that for the opposite case of $\lambda\mathbf{T}(0) \ll 1$ we have $V_0 \approx \lambda^2/\omega_0$. This is the dilute dyonic density limit which is not our case. The dyon ensemble in the center symmetric phase is dense [1]. In

terms of (34) all equations can be solved analytically. However, we have checked that their accuracy is limited. All the analysis to follow will be carried out exactly without these estimates.

B. Gap equation

The free energy depends on two parameters, the mean values of λ and Σ fields, which should be chosen at the minimum of it. The equations following from vanishing first derivatives are known in literature as the "gap equations." It is useful, to recast it in terms of the integral V_0 defined above. In particular, we have

$$\Sigma = \frac{4V_0^2}{\alpha^2} = \frac{2V_0}{\lambda}, \tag{35}$$

while the effective potential (32) is

$$-\mathcal{V}/\mathbb{V}_3 = 2V_0 + \int \frac{d^3p}{(2\pi)^3} \ln\left(1 + \frac{M^2(p)}{p^2}\right). \tag{36}$$

We have introduced the momentum-dependent constituent quark mass $M(p)$ as

$$M(p) = \lambda p \mathbf{T}(p) = \frac{\alpha^2}{2V_0} p\mathbf{T}(p), \tag{37}$$

which is seen to vanish linearly at $p/\omega_0 \ll 1$ and as $1/p^2$ for $p/\omega_0 \gg 1$. In Fig. 1 we show the behavior of the dimensionless mass ratio $TM(p)/\lambda$ as a function of p/T. Equations (7) through (33) obey the gap equation for the λ parameter,

$$\int \frac{d^3p}{(2\pi)^3} \frac{M^2(p)}{p^2 + M^2(p)} = \frac{n_D}{4}, \tag{38}$$

relating the integral we called V_0 to the dyonic density n_D. So given n_D, the solution to the gap equation (39) fixes λ and, thus, the quark constituent mass $M(p)$ and, therefore, through the delta-function constraint in (25), the value of Σ.

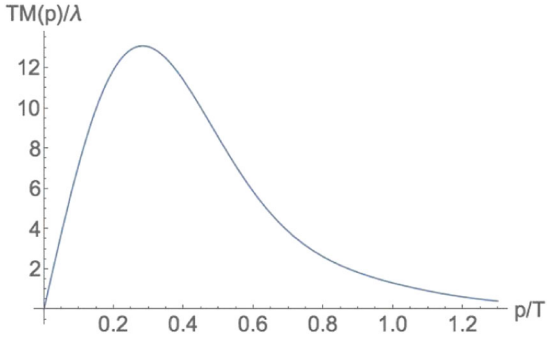

FIG. 1 (color online). The momentum-dependent quark constituent mass $TM(p)/\lambda$ versus p/T.

In our approach the n_D is not an external input, but should itself be calculated from the derivatives of the free energy; e.g., the M-dyon density is

$$n_M = \frac{1}{2}\frac{\partial(-\mathcal{V}/\mathbb{V}_3)}{\partial \ln f_M} = \int \frac{d^3p}{(2\pi)^3} \frac{M^2(p)}{p^2 + M^2(p)} = V_0. \tag{39}$$

Since $n_D = n_M + n_L + n_{\tilde{M}} + n_{\tilde{L}} = 4n_M$ as all partial dyonic densities are equal in the confined phase, we have $V_0 = n_D/4$.

C. Chiral condensate

The nonvanishing of Σ signals the nonvanishing of the chiral condensate $\langle \bar{q}q \rangle$ and, therefore, the spontaneous breaking of chiral symmetry. Standard demonstration of that is done via introduction of a nonzero but small light quark mass m, which changes (18) to

$$\prod_i [-\psi_1^\dagger \psi_1(x_{Li}) + m] \prod_j [-\psi_2^\dagger \psi_2(y_{\bar{L}j}) + m]. \tag{40}$$

A rerun of the bosonization scheme with (40) shows that only one contribution in (29) is now shifted,

$$8\pi\sqrt{f_L f_M \Sigma/2} \to 8\pi\sqrt{f_L f_M(\Sigma/2 + m)}, \tag{41}$$

changing the saddle point solutions (31) to

$$\lambda = \frac{\alpha}{\sqrt{\Sigma + 2m}} \tag{42}$$

and (33) to

$$\frac{\alpha^2}{2\lambda} - m\lambda = \int \frac{d^3p}{(2\pi)^3} \frac{\lambda^2 \mathbf{T}^2(p)}{1 + \lambda^2 \mathbf{T}^2(p)}. \tag{43}$$

The effective potential is now

$$-\mathcal{V}/\mathbb{V}_3 = \frac{\alpha^2}{\lambda} + 2m\lambda + \int \frac{d^3p}{(2\pi)^3} \ln\left(1 + \lambda^2 \mathbf{T}^2(p)\right). \tag{44}$$

Inserting (44) in the general definition of the chiral condensate in the saddle point approximation,

$$\frac{\langle \bar{q}q \rangle}{T} = \frac{\partial(\mathcal{V}/\mathbb{V}_3)}{\partial m}, \tag{45}$$

and using the gap equation, we obtain

$$\frac{\langle \bar{q}q \rangle}{T} = -2\lambda. \tag{46}$$

We have used that α is independent of m and that the contribution multiplying $\partial\lambda/\partial m$ is zero thanks to the gap equation. In the chiral limit, λ is fixed by the solution of the gap-equation (38) for the constituent quark mass and the

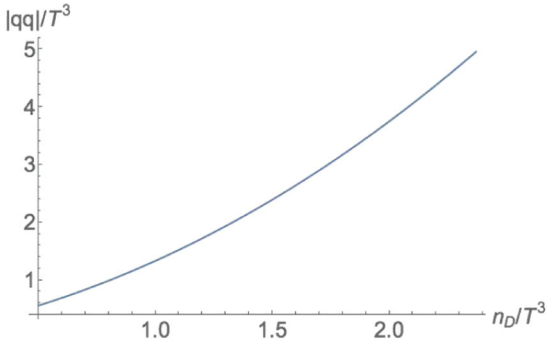

FIG. 2 (color online). The absolute value of the (dimensionless) quark condensate $|\langle\bar{q}q\rangle|/T^3$ versus the (dimensionless) dyon density n_D/T^3.

dyon density n_D. It is therefore an implicit function of n_D, i.e. $\lambda \equiv \lambda[n_D]$.

The use of (3) into (38) leads to only numerical results for λ and thus $M(p)$. In Fig. 2 we show the behavior of the absolute value of the quark condensate $|\langle\bar{q}q\rangle|/T^3$ versus the dyon density n_D/T^3. Note that $|\langle\bar{q}q\rangle|/T^3$ decreases with decreasing dyon density. In this range, a best fit gives

$$\frac{|\langle\bar{q}q\rangle|}{T^3} \approx 1.25\left(\frac{n_D}{T^3}\right)^{1.63}. \tag{47}$$

For analytical estimates, we note that we can always select a temperature in the range $0.5 < T_0 < T_c$ for which the chiral condensate is $|\bar{q}q|/T_0^3 = 1$ at that temperature. From (46) we have $\lambda_0 = T_0^2/2$ in the chiral limit. Inserting this value for $M(p)$ in (38) shows that the corresponding dyon density at $T = T_0$ is $n_0/T_0^3 = 0.80$.

D. Screened Polyakov lines

As we noted earlier in (28), the spontaneous breaking of chiral symmetry with a finite value of $\Sigma/2$ still preserves center symmetry with $v_l = v_m = 1/2$. However, strict confinement is lost because of screening. Heavy fundamental color charges are now screened by the light constituent quarks through the formation of tightly bound heavy-light and colorless mesons. The bound mesons are blind to the Z_2 center and, thus, to the holonomies, now with

$$\langle L(x)\rangle \approx e^{-\beta(\Sigma/2+m+\mathcal{O}(\alpha_s))}. \tag{48}$$

The $\mathcal{O}(\alpha_s)$ contribution in (48) is UV sensitive and requires a specific subtraction. Using (46) together with (35) and (38) where $N_c = 2$, we can recast (48) in the chiral limit into the generic relation

$$n_D \approx N_c\langle\bar{q}q\rangle \ln(\langle L(x)\rangle)(1+\mathcal{O}(\alpha_s)) \tag{49}$$

for the dyonic density in the range $0.5 < T < T_c$. Equation (49) provides for an independent estimate of the dyon density in unquenched QCD. Finally, we note that for a large separation, the correlation of two Polyakov lines clusters,

$$\langle L^\dagger(x)L(0)\rangle \approx |\langle L(0)\rangle|^2 \approx e^{-\beta(\Sigma+2m+\mathcal{O}(\alpha_s))}, \tag{50}$$

with a vanishing of the electric string tension due to light quark screening.

IV. MESONIC SPECTRUM

The stability of the vacuum solution with $N_f = 1$ can be tested by fluctuating in the fermionic channel which consists of both a scalar σ meson and a pseudoscalar η' meson. Both are massive—the former through the spontaneous breaking of chiral symmetry with finite Σ, while the latter through the $U_A(1)$ anomaly with a finite topological susceptibility. The mesonic spectrum for general N_f is detailed in Appendix C.

A. Sigma meson

A simple way to probe the scalar spectrum is to note that in the spontaneously broken state, the fermion kinetic contribution in (22) is now

$$\begin{pmatrix} 0 & \mathbf{G}(x,y) \\ -\mathbf{G}(x,y) & 0 \end{pmatrix} \to \begin{pmatrix} i\lambda\mathbf{1}_{xy} & \mathbf{G}(x,y) \\ -\mathbf{G}(x,y) & i\lambda\mathbf{1}_{xy} \end{pmatrix}, \tag{51}$$

with $\mathbf{1}_{xy} = \delta^3(x-y)$. The scalar meson in the long wavelength limit can be identified with the fluctuations in the chiral condensate through $i\lambda$ in (51) or

$$i\lambda \to i\lambda_0 + i\delta\lambda \equiv i\lambda_0\left(1+\frac{\sigma_s}{f_s}\right) \tag{52}$$

with $\lambda_0 = -\langle\bar{q}q\rangle/2T$ in the chiral limit. Fluctuations in λ also induce fluctuations in Σ. Thus, consistency requires

$$\Sigma \to \Sigma_0 + \delta\Sigma. \tag{53}$$

Inserting (52) into (51) and (53) into the delta-constraint (25) allows for a derivation of the effective action for the fluctuating parts $\delta\Sigma, \delta\lambda$. The linear contributions are zero by the saddle point equations. So the net contributions are quadratic and higher. In leading quadratic order $\delta\Sigma, \delta\lambda$ mix,

$$\begin{aligned}\mathbf{S}_2[\delta\lambda,\delta\Sigma] = &-\frac{1}{2}\int\frac{d^3p}{(2\pi)^3}(-2i)\delta\Sigma(p)\delta\lambda(-p)\\ &-\frac{1}{2}\int\frac{d^3p}{(2\pi)^3}\frac{n_D}{4\Sigma_0^2}\delta\Sigma(p)\delta\Sigma(-p)\\ &-\frac{1}{2}\int\frac{d^3p}{(2\pi)^3}\delta\lambda(p)\mathbf{G}_s^{-1}(p)\delta\lambda(-p)\end{aligned} \tag{54}$$

with

$$\mathbf{G}_s^{-1}(p) = \int \frac{d^3q}{(2\pi)^3} \frac{2(-\lambda_0^2 + \mathbf{G}(q^2)\mathbf{G}(p+q)^2)}{(\mathbf{G}^2(q^2)+\lambda_0^2)(\mathbf{G}^2(q+p)^2)+\lambda_0^2)}. \tag{55}$$

To undo the mixing in (55), we solve for $\delta\Sigma$ to leading order,

$$-2i\delta\lambda - \frac{n_D}{2\Sigma_0^2}\delta\Sigma = 0, \tag{56}$$

and insert it back into (55) to give finally the quadratic action for the scalar meson,

$$\mathbf{S}_2[\sigma_s] = +\frac{1}{2f_s^2}\int \frac{d^3p}{(2\pi)^3}\sigma_s(p)\Delta_+(p)\sigma_s(-p), \tag{57}$$

with

$$\Delta_+(p) = \lambda_0^2\mathbf{G}_s^{-1}(p) + n_D. \tag{58}$$

The kernel in (58) can be further reduced using the gap equation for n_D. Thus,

$$\Delta_+(p) = \frac{n_D}{2} + \int \frac{d^3q}{(2\pi)^3}\frac{(M_+q_- + M_-q_+)^2}{(M_+^2+q_+^2)(M_-^2+q_-^2)} \tag{59}$$

Here, $M_\pm = M(q_\pm)$ and $p_\pm = q \pm p/2$, where $M(q)$ is the running constituent mass in (37). For $N_f = 1$ we have mixing between the scalar as a $\bar{q}q$ quark state and the scalar glueball. The $n_D/2$ contribution in (59) is just the mixing contribution, while the second contribution is clearly the $\bar{q}q$ quark bubble contribution. A similar mixing in the scalar sector was observed in the instanton liquid model of the QCD vacuum [22].

A comparison of the small momentum expansion of (57) after subtraction of the $n_D/2$ glue mix yields the canonical scalar action in x space,

$$\mathbf{S}_2[\sigma_s] \equiv +\frac{1}{2T}\int d^3x(|\nabla\sigma_s|^2 + m_s^2\sigma_s{}^2) \tag{60}$$

with

$$m_s^2 f_s^2 = T\int \frac{d^3q}{(2\pi)^3}\frac{4q^2M^2(q)}{(q^2+M^2(q))^2}. \tag{61}$$

In Fig. 3 we show the behavior of $m_s^2f_s^2/T^4$ from (61) as a function of the scaled dyon density n_D/T^3. Increasing density amounts to lower temperature, with a transition density expected around 1.

B. Eta′ meson

To generate the effective quadratic action for the η' meson, we need to fluctuate asymmetrically around the chiral condensate in (51):

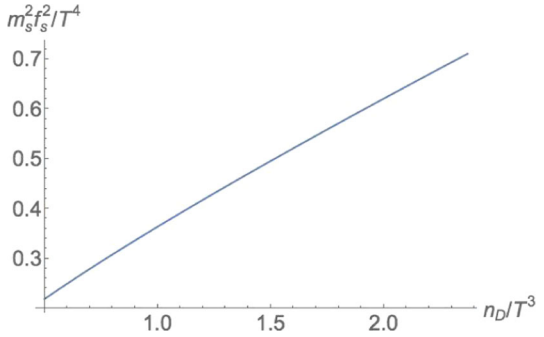

FIG. 3 (color online). $m_s^2f_s^2/T^4$ versus the dyon density n_D/T^3.

$$i\lambda \to i\lambda_\pm \equiv i\lambda_0\left(1 \pm \frac{i\eta}{\sqrt{2}f_\eta}\right). \tag{62}$$

A rerun of the preceding arguments for the scalar meson yields

$$\mathbf{S}_2[\eta] = -\frac{1}{2f_\eta^2}\int \eta(p)\Delta_-(p)\eta(-p) \tag{63}$$

with

$$\Delta_-(p) = \frac{\alpha^2}{\lambda_0^2} - \int \frac{d^3q}{(2\pi)^3}\frac{M_+M_-(M_+M_- + q_+q_-)}{(q_+^2+M_+^2)(q_-^2+M_-^2)} \tag{64}$$

for arbitrary current mass m. Using the gap equation for n_D for nonzero m, we may further reduce (64) into

$$\Delta_-(p) = 2m\lambda + \frac{n_D}{4} + \frac{1}{2}\int \frac{d^3q}{(2\pi)^3}\frac{(q_+M_- - q_-M_+)^2}{(q_+^2+M_+^2)(q_-^2+M_-^2)}. \tag{65}$$

Since $T\Delta_-(0) \equiv f_\eta^2 m_\eta^2$, it follows that

$$f_\eta^2 m_\eta^2 = -m\langle\bar{q}q\rangle + \chi_T \tag{66}$$

with $\chi_T = Tn_D/4$. The first contribution in (70) is the Gell-Mann-Oakes-Renner contribution to the η' mass as a would-be Goldstone boson, while the second contribution is a Witten-Veneziano-like contribution. It suggests an unquenched topological susceptibility of $\chi_T = Tn_D/4$ as opposed to the quenched topological susceptibility [1]. In the chiral limit with $m = 0$,

$$f_\eta^2 m_\eta^2 \approx \chi_T \equiv \frac{Tn_D}{4}. \tag{67}$$

Since the topological susceptibility for dyons $\chi_T \approx \mathcal{O}(N_c^0)$ and $f_\eta^2 \approx \mathcal{O}(N_c)$, the η' mass is seen to vanish at large N_c. In Fig. 4 we display the ratio of the squared scalar to pseudoscalar mass as a function of the scaled dyon density n_D/T^3 assuming $f_s \approx f_\eta$ by chiral symmetry. The ratio

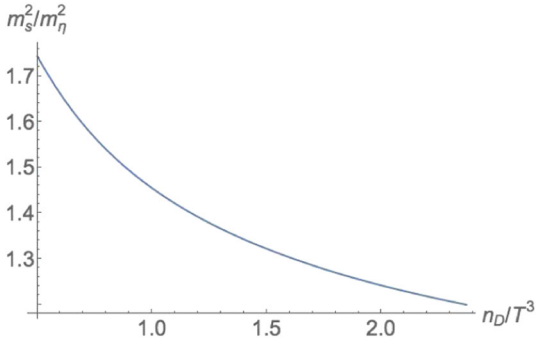

FIG. 4 (color online). The mass ratio squared, for scalar to pseudo-scalar mesons m_s^2/m_η^2, versus the (dimensionless) dyon density n_D/T^3, assuming $f_s \approx f_\eta$ (see text).

decreases with increasing dyon density or lower temperature. This ratio may be compared to the value in the QCD vacuum, i.e. $T = 0, N_c = 3, N_f = 2 + 1$, which is about $1/2$. Going in the opposite direction, to smaller densities, note that the expected phase transition density is around 1.

A simple but approximate understanding of (66) follows by noting that (25) is $\mathrm{U}(1)_V$ symmetric but upsets $\mathrm{U}(1)_A$ symmetry through the fermionic contributions. Under $\mathrm{U}(1)_A$ with $\psi \to e^{i\gamma_5\theta/2}\psi$, the fermionic contributions in (27) change:

$$+2\pi f_L e^{i\theta} v_l \psi^\dagger \gamma_+ \psi e^{w_L - w_M} + 2\pi f_{\bar{L}} e^{-i\theta} v_l \psi^\dagger \gamma_- \psi e^{w_{\bar{L}} - w_{\bar{M}}}. \tag{68}$$

This amounts to shifting $f_{L,\bar{L}} \to f_{L,\bar{L}} e^{\pm i\theta}$ in the parity symmetric effective potential (30). An estimate of mass of the η' follows by identifying $\theta/2 \to \eta/f_\eta/\sqrt{2}$ with a constant η' field. So the η' mass is related to the topological susceptibility χ_T. Specifically, the pertinent contribution from the effective potential (30) is now

$$-\mathcal{V}/\mathbb{V}_3 \to 4\pi (f_L f_M (\Sigma/2 + m))^{1/2} \cos(\sqrt{2}\eta/f_\eta), \tag{69}$$

where we have retained the small quark mass m. Expanding (69) yields the quadratic contribution,

$$-\frac{T}{2}\left(\frac{m2\alpha}{\sqrt{\Sigma} f_\eta^2} + \frac{2\alpha\sqrt{\Sigma}}{f_\eta^2}\right)\eta^2. \tag{70}$$

Recall that $\alpha = 4\pi\sqrt{f_M f_L/2}$. From (46) we have $2\alpha/\Sigma = -\langle\bar{q}q\rangle$, and from (35) we have $\alpha\sqrt{\Sigma} = 2V_0 = n_D/2$. The squared η' mass follows as in (66) but with an incorrect $4\chi_T$ contribution.

V. DYON PAIRING THROUGH FERMION EXCHANGES

Above the temperature of the chiral phase transition, $T > T_\chi$, there is no quark condensate, and dyons and antidyons pair into neutral "dyon-antidyon molecules" bound through fermion exchanges [15], a situation somewhat reminiscent of the BKT transition [7,8].

This can be seen by noting that the chiral matrix $\tilde{\mathbf{T}}$ in (7) is banded with a band range set by the inverse temperature,

$$\mathbf{T}_{ij} \approx \mathbf{t}_f e^{-\frac{1}{2}\omega_0|x_i - y_j|} \to \mathbf{t}_f \delta_{ij}. \tag{71}$$

With increasing temperature, the range of $\tilde{\mathbf{T}}$ is reduced to the nearest neighbor. As a result, the hopping is stalled with

$$|\det \tilde{\mathbf{T}}| \to |\mathbf{t}_f|^{K_L + K_{\bar{L}}} \delta_{K_L K_{\bar{L}}}.$$

The light quark spectrum is now gapped at $\lambda_\pm = \pm|\mathbf{t}_f|$ with a vanishing chiral condensate $\langle\bar{q}q\rangle = 0$. An estimate of the hopping parameter follows from

$$\mathbf{t}_f \equiv \int \frac{d^3p}{(2\pi)^3} \mathbf{T}(p) \approx 0.8\omega_0, \tag{72}$$

using (8)–(A1) and Parseval equality.

A simple but crude estimate of the transition density at which the pairing into molecules overtakes the chirally broken phase is when the molecular gap becomes larger than Σ, thus restoring chiral symmetry. Σ characterizes the size of the delocalized zero mode zone. Using (72) this occurs for $|\mathbf{t}_f| \approx 2.51T \approx \Sigma$. Since $\Sigma/T = n_D/|\langle\bar{q}q\rangle|$, this means a transition when $|\langle\bar{q}q\rangle|/n_D \approx 1/2.5$. From the numerical fit (47), this estimate yields to a chiral restoration for a dilute dyon ensemble with

$$\frac{n_D}{T^3} < \frac{n_\chi}{T^3} \approx 0.16. \tag{73}$$

Near the transition temperature, a substantial amount of dyons can already be paired, resulting in a weakening of the chiral condensate.

In terms of (71), the partition function (1) is highly correlated. The result after summing over pairs is

$$\mathcal{Z}_{\mathrm{mol}}[T] = \int D[b]D[\sigma]D[\chi]D[w] e^{-S_0 - S_M} \times |\mathbf{t}_f|\sqrt{F_L F_{\bar{L}}} I_2(|\mathbf{t}_f|\sqrt{F_L F_{\bar{L}}}), \tag{74}$$

with S_0 defined in (9)–(11) and S_M defined in (12) for only M and $\bar{M}$. The argument of the modified Bessel function I_2 is composed of

$$F_L = \int d^3x e^{+b-i\sigma+w_L-w_M} \times f_L(4\pi v_l + |\chi_L - \chi_M|^2 + v_L - v_M)$$
$$F_{\bar{L}} = \int d^3x e^{+b+i\sigma+w_{\bar{L}}-w_{\bar{M}}} \times f_{\bar{L}}(4\pi v_{\bar{l}} + |\chi_{\bar{L}} - \chi_{\bar{M}}|^2 + v_{\bar{L}} - v_{\bar{M}}). \quad (75)$$

The molecular partition function in (74) is highly nonlinear in the auxiliary fields. For large $|\mathbf{t}_f|$, we may use the asymptotic form of $I_2(z) \approx e^z/\sqrt{2\pi z}$ in (75) and linearize the argument of the modified Bessel function:

$$\sqrt{F_L F_{\bar{L}}} \approx \frac{F_L + F_{\bar{L}}}{\sqrt{2}}\left(1 - \frac{F_L^2 + F_{\bar{L}}^2}{2(F_L + F_{\bar{L}})^2}\right). \quad (76)$$

As a first step to be justified below, we may drop the nonlinear contributions in (76) and the preexponent in (74) to have

$$\mathcal{Z}_{\rm mol}[T] \approx \int D[b]D[\sigma]D[\chi]D[w]e^{-S_0 - S_M + (\tilde{F}_L + \tilde{F}_{\bar{L}})/\sqrt{2}} \quad (77)$$

after rescaling $f_{L,\bar{L}} \to f_{L,\bar{L}}|\mathbf{t}_f|/\sqrt{2}$ in $\tilde{F}$. Equation (77) is now analogous to the SU(2) Yang-Mills partition function [1,3] with the new rescaled fugacities. A rerun of the arguments in this case shows that the ground state is still center symmetric. However, the ground state is chirally symmetric. It is worth noting that this state is parity even, so the neglected nonlinear corrections in (76) amount to $(1 - 1/4)$ which is about a 25% reduction in the pertinent pressure contribution which is then

$$\mathcal{P}_{\rm mol} = \frac{\ln \mathcal{Z}_{\rm mol}}{V_3/T} \approx 8\pi T\left(\frac{f_M f_L |\mathbf{t}_f|}{\sqrt{2}}\right)^{1/2}. \quad (78)$$

VI. HIGHER NUMBER OF COLORS AND FLAVORS

The extension of the current analysis to many N_c colors and N_f massless flavors is straightforward in principle. For finite N_c, the KvBLL instanton splits into N_c constituent dyon with $1/N_c$ topological charge and fugacity f_l with $1 \le l \le N_c$. The L-dyon zero mode which is antiperiodic is now carried by the $l = N_c$ constituent dyon. The net effect is a change in the fermionic contribution in (25) through $\mathbf{G} \to \mathbf{G} \otimes \mathbf{1}_f$ and a change in the parity even effective potential (27) as

$$-\mathcal{V}/\mathbb{V}_3 \to + i\lambda N_f \Sigma + 4\pi f_i v_i (e^{w_{i+1}-w_i} + e^{w_{\tilde{i}+1}-w_{\tilde{i}}}) + 4\pi f_{N_c} v_{N_c} \frac{1}{N_f!}\det{}_{N_f}(\psi_l^\dagger \gamma_+ \psi_g) e^{w_{N_c}-w_{N_c+1}} + 4\pi f_{\bar{N}_c} v_{\bar{N}_c} \frac{1}{N_f!}\det{}_{N_f}(\psi_l^\dagger \gamma_- \psi_g) e^{w_{\bar{N}_c}-w_{\bar{N}_c+1}}, \quad (79)$$

where the implicit i summation is over $i = 1, \ldots, N_c - 1$. The potential $\mathcal{V}$ has manifest $\mathrm{SU}(N_f)_V \times \mathrm{SU}(N_f)_A \times \mathrm{U}(1)_V$ flavor symmetry. As a result, the parity even effective potential (30) after pertinent bosonization and Fierzing yields

$$-\mathcal{V}/\mathbb{V}_3 \to + i\lambda N_f \Sigma + 2\alpha(N_c)\Sigma^x + N_f \int \frac{d^3p}{(2\pi)^3} \ln(1 - \lambda^2 \mathbf{T}^2(p)), \quad (80)$$

with $x = N_f/N_c$ and $\alpha(N_c) = 4\pi f(N_c)/2^x$. The mean fugacity is

$$f(N_c) = (f_1 \ldots f_{N_c})^{1/N_c}. \quad (81)$$

We note that its scaling with N_c follows from the scaling of each fugacity by semiclassics, i.e., $f_i \approx 1/\alpha_s^2$. Thus,

$$f(N_c) \approx N_c^{2N_c/N_c} \approx N_c^2, \quad (82)$$

so that $\alpha(N_c) \approx N_c^2$.

A. Gap equation and chiral condensate

For general $x = N_f/N_c$, the saddle point equation in Σ of (80) gives

$$\Sigma = \left(\frac{\tilde{\lambda}}{2x\alpha(N_c)}\right)^{\frac{1}{x-1}} \quad (83)$$

after the shift $-i\lambda \to \lambda$ and $\tilde{\lambda} = N_f\lambda$. Inserting (83) into (80) yields

$$-\mathcal{V}/\mathbb{V}_3 = -2\alpha(N_c)(x-1)\left(\frac{\tilde{\lambda}}{2x\alpha(N_c)}\right)^{\frac{x}{x-1}} + xN_c \int \frac{d^3p}{(2\pi)^3} \ln\left(1 + \frac{\tilde{\lambda}^2}{N_f^2}\mathbf{T}^2(p)\right), \quad (84)$$

The case $x = 1$ is special. The effective potential in (80) is linear in Σ with no *a priori* saddle point along Σ. We have checked that taking the saddle point in $\tilde{\lambda}$ first and then the saddle point in Σ after the substitution results in the same gap equation to follow. Also, it can be checked explicitly that the same results follow by taking the limit $x \to 1$.

The effective potential (84) has different shapes depending on the ratio of the number of flavors to the number of colors x. Let us explain that in detail for four cases:

(i) If $x < 1$, the first term in (84) has a positive coefficient and a negative power, so it is decreasing at small $\tilde{\lambda}$. At large value of $\tilde{\lambda}$, the second term is growing as $\ln\tilde{\lambda}$. Thus, a minimum in between must exist. This minimum is the physical solution we are after.

(ii) If $1 < x < 2$, the coefficient of the first term is negative but its power is now positive. So, again, there is a decrease at small $\tilde{\lambda}$ and, thus, a minimum.

(iii) If $x > 2$, the leading behavior at small $\tilde{\lambda}$ is now dominated by the second term which goes as $\tilde{\lambda}^2$ with a positive coefficient. One may check that the potential is monotonously increasing for any $\tilde{\lambda}$ with no extremum. There is no gap equation, which means chiral symmetry cannot be broken in the mean-field approximation.

(iv) If $x = 2$, there are two different contributions of opposite sign to order $\tilde{\lambda}^2$ at small $\tilde{\lambda}$. An extremum forms only if the following condition is met:

$$\int \frac{d^3p}{(2\pi)^3}\mathbf{T}^2(p) < \frac{N_c}{4\alpha(N_c)} = \mathcal{O}\left(\frac{1}{N_c}\right). \quad (85)$$

Using the exact form (A3) and the solution to the gap equation at $T = T_0$, we have

$$\int \frac{d^3p}{(2\pi)^3}\mathbf{T}^2(p) = \frac{10.37}{T_0}, \quad (86)$$

which shows that (85) is, in general, upset, and this case does *not* possess a minimum.

With this in mind and for $x < 2$, the extremum of (84) in $\tilde{\lambda}$ yields the gaplike equation

$$\left(\frac{\tilde{\lambda}}{2x\alpha(N_c)}\right)^{\frac{x}{x-1}} = \frac{N_c V_{N_f-1}}{\alpha(N_c)}, \quad (87)$$

with the new identification

$$V_{N_f-1} \equiv \int \frac{d^3p}{(2\pi)^3}\frac{\frac{\tilde{\lambda}^2}{N_f^2}\mathbf{T}^2(p)}{1+\frac{\tilde{\lambda}^2}{N_f^2}\mathbf{T}^2(p)}. \quad (88)$$

The dyonic density is now identified with

$$n_D = 2N_c\frac{1}{2}\frac{\partial(-\mathcal{V}/\mathbb{V}_3)}{\partial\ln f_M} = 2N_c V_{N_f-1}. \quad (89)$$

In terms of (88)–(89) the running constituent mass $M(p) = (\tilde{\lambda}/N_f)p\mathbf{T}(p)$ obeys the gap equation

$$\int \frac{d^3p}{(2\pi)^3}\frac{M^2(p)}{p^2+M^2(p)} = \frac{n_D}{2N_c}. \quad (90)$$

From (87) it follows that $V_{N_f-1} \approx N_c$ and, therefore, $n_D \approx N_c^2$. The dyonic description we have reached is consistent with large N_c counting. Since $n_D \approx N_c^2 \gg 1$, crystallization in the form of dyonic salt is expected at large N_c [23].

For $x < 2$, the center symmetric vacuum also breaks spontaneously chiral symmetry, with a vacuum condensate given by

$$\frac{\langle\bar{q}q\rangle}{T} = -2\tilde{\lambda}_0, \quad (91)$$

where $\tilde{\lambda}_0$ is the value of $\tilde{\lambda}$ in the chiral limit. Since $\tilde{\lambda}_0 \approx N_f N_c$, the chiral condensate in (91) is of order $N_f N_c$ as expected.

To summarize, chiral restoration as well as the loss of center symmetry occur simultaneously for $x_\chi \geq 2$ as per our result in (29). This value of $x = N_f/N_c$ is close to the critical value of $x_\chi = 5/3$ originally suggested in the instanton liquid model in the first reference in [14]. First simulations of the dyon ensemble with $N_c = 2$ [18] also indicate that the border line seems to be $N_f = 4$, in agreement with $x_\chi \approx 2$.

Current lattice data are summarized, e.g., in Fig. 5 of [24] for $N_c = 3$. Indeed, they seem to indicate a change in the value of the chiral transition temperature (in units of the vacuum string tension) $T_\chi/\sqrt{\sigma}$ at $x = 2$ or $N_f = 6$, but instead of vanishing, this ratio remains flat up to $N_f = 8$. For such a large N_f the number of quark lines $2N_f$ connected to an L dyon is large. Maybe the correlations between them are too strong for the mean-field approximation to remain valid.

The chiral transition we have discussed in this section should not be confused with another phase transition in theories with a large number of flavors, namely, the conformal (fixed infrared coupling) phase. The reported lattice [25] and holographic (Veneziano limit) [26] results put this conformal transition at a much larger number of flavors $x_{\text{conformal}} \approx 4$, or $N_f = 12$ for $N_c = 3$.

B. Thermodynamics of dyonic phase with $x \leq 1$

In the presence of light quarks, the total thermodynamical pressure of the dyon-antidyon liquid consists of the classical and nonperturbative contributions in (80) at the extremum, plus its perturbative correction for finite and symmetric holonomies $v = 1/N_c$ [13], plus the purely perturbative black-body contribution (ignoring the higher-order $\mathcal{O}(\alpha_s)$ quantum corrections). Identifying the classical pressure with $-\mathcal{V}/\beta V_3$ with $\beta = 1/T$, we have

$$\frac{\mathcal{P}_{\rm tot}-\mathcal{P}_{\rm per}}{N_cT^4} = +(1-x)\tilde{n}_D + \frac{x}{T^3}\int\frac{d^3p}{(2\pi)^3}\ln\left(1+\frac{M^2(p)}{p^2}\right) \quad (92)$$

with $\tilde{n}_D = n_D/(N_cT^3)$. The assessment of the logarithmic integral follows by numerical integration using the explicit form of $M(p)$ and the solution to the gap equation. The result is linear in the reduced dyon density for small and asymptotic densities,

$$\frac{1}{T^3}\int\frac{d^3p}{(2\pi)^3}\ln\left(1+\frac{M^2(p)}{p^2}\right) \approx \kappa(\tilde{n}_D)\tilde{n}_D, \quad (93)$$

with $\kappa(\tilde{n}_D \ll 1)\approx 1$ and $\kappa(\tilde{n}_D \gg 1)\approx 2$. A simple interpolation to the overall numerical results is

$$\kappa(\tilde{n}_D) \approx \frac{1+2\frac{\tilde{n}_D}{10}}{1+\frac{\tilde{n}_D}{10}}. \quad (94)$$

Since $\tilde{n}_D \approx \mathcal{O}(N_c)$, large density corresponds to large N_c with $\kappa \approx 2$, modulo crystallization. In Fig. 5 we display (93) as a function of the reduced dyon density $\tilde{n}_D$ at intermediate densities. The linearity of the logarithm in $\tilde{n}_D$ both at small and asymptotic dyon densities follows from the scaling of $V_0 = n_D/2N_c$ with λ as discussed in (34).

In terms of (93) the classical pressure contribution in (92) simplifies to

$$\frac{\mathcal{P}_{\rm tot}-\mathcal{P}_{\rm per}}{N_cT^4} \approx (1-x(1-\kappa))\tilde{n}_D, \quad (95)$$

with $1 \le \kappa \le 2$. In the quenched limit or $x = 0$, it reduces to the dyonic result obtained for the pure Yang-Mills analysis in [1], ignoring the Debye-Huckel corrections. The fermion-induced interactions in the center symmetric phase increase the pressure away from the free limit for $0 < x \le 1$. Remarkably, for small densities $(1-\kappa)\approx 0$ and Eq. (95) with fermions is close to a free ensemble of dyons. For large densities or large N_c, $(1-\kappa)\approx -1$ and Eq. (95) with fermions is more repulsive than the free dyon ensemble.

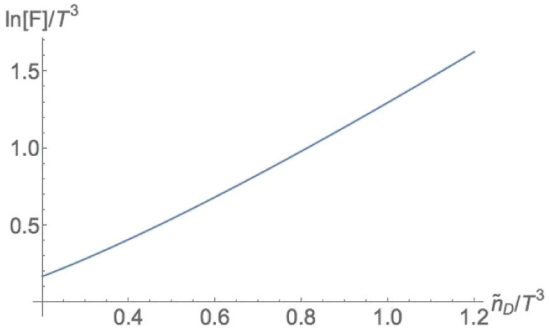

FIG. 5 (color online). The fermionic loop $\ln[F]/T^3$ versus the reduced dyon density $\tilde{n}_D/T^3$. See text.

The perturbative contribution is given by

$$\frac{\mathcal{P}_{\rm per}}{T^4} \approx -\frac{\pi^2}{45}\left(N_c^2-\frac{1}{N_c^2}\right)+\frac{\pi^2}{45}(N_c^2-1) - \frac{7\pi^2 x}{180}\left(N_c^2-\frac{1}{N_c^2}\right)+\frac{7\pi^2 x}{180}N_c^2. \quad (96)$$

The first contribution is the free gluon contribution in the symmetric phase with $v = 1/N_c$. The second contribution is the free black-body gluon contribution, which is cancelled by the second contribution in leading order in $1/N_c$ in the symmetric phase [3]. The third contribution is the free quark contribution in the symmetric phase with $v = 1/N_c$. The fourth and last contribution is the black-body quark contribution, which we note is cancelled by the third contribution in leading order in $1/N_c$. This generalizes the observation in [3] to QCD.

An estimate of the transition temperature T_c from the symmetric phase with $v = 1/N_c$ to the asymmetric phase with $v = 0$ follows when all the non-black-body contributions in the total pressure $\mathcal{P}_{\rm tot}$ cancel out. This occurs when the rescaled dyon density $\mathbf{n}_D = n_D/(N_c^2T^3)$ solves

$$\mathbf{n}_{Dc} \approx \frac{\pi^2}{45}\left(1-\frac{1}{N_c^4}\right)\frac{1+\frac{7x}{4}}{1+x(\kappa(\mathbf{n}_{Dc})-1)} \quad (97)$$

with again $1 \le \kappa(\mathbf{n}_{Dc}) \le 1$.

C. Thermodynamics of molecular phase

For completeness we note that near the chiral transition most of the $L\bar{L}$ dyons start to pair into molecules, for which case the total pressure is more appropriately described by

$$\frac{\mathcal{P}_{\rm tot,mol}-\mathcal{P}_{\rm per}}{T^4} \approx \frac{2\tilde{\Lambda}^4}{\alpha_s^2}\left(\frac{|\tilde{\mathbf{t}}_f|^{N_f}}{\sqrt{2}}\right)^{\frac{1}{2}}, \quad (98)$$

with $|\tilde{\mathbf{t}}_f| = |\mathbf{t}_f|/\Lambda$. Here, the scale parameter $\tilde{\Lambda} = \Lambda/T$ is identified with the vacuum dyon density $n_D \to 2\Lambda^4/\alpha_s^2 T$ as in [3]. We note that for $N_f \to 0$, (98) is off by $2^{-\frac{1}{4}}$ in the ground state pressure from the Yang-Mills limit in [3]. This can be traced back to our linearized approximation in (76). The critical temperature is now

$$T_c \approx \frac{2\Lambda}{\sqrt{\tilde{\alpha}_s}}\left(\frac{|\tilde{\mathbf{t}}_f|^{N_f}}{\sqrt{2}}\right)^{\frac{1}{8}}\frac{1}{h^{\frac{1}{4}}(x)}, \quad (99)$$

with $\tilde{\alpha}_s = N_c\alpha_s$, and

$$h(x) = \frac{\pi^2}{45}\left(1+\frac{7x}{4}\right)\left(1-\frac{1}{N_c^4}\right). \quad (100)$$

Equation (99) characterizes the transition from a center symmetric but chirally symmetric phase to a center asymmetric and chirally symmetric phase. Which transition is likely to occur first can be estimated by comparing the total liquid pressure in (92) to the total molecular pressure in (98). This is best addressed using mixtures.

VII. CONCLUSIONS

We have extended the mean-field treatment of the SU(2) dyon-antidyon liquid in [1], to account for light quarks. Anti-periodic fundamental quarks develop zero modes for the $L, \bar{L}$ dyons only. In the dense phase under consideration with $T < T_c$, these zero modes are collectivized into a zero mode zone of quasizero modes which dominates the low-eigenvalue part of the Dirac spectrum. This phenomenon is analogous to the one used in the instanton liquid model [14], although the zero modes themselves and most of the results are different. The important interplay between center symmetry and the spontaneous breaking of chiral symmetry which is absent in [14] is now clarified. In particular, we have explicitly shown how the chiral effective Lagrangian for light quarks knows about confinement.

In the infrared, the fermionic determinant is entirely saturated by these quasizero modes [15], modifying the dyon-antidyon measure initially suggested in [3,6] to include light quarks. For the $N_f = 1$ case of one massless quark, we have shown that the fermionic determinant modifies the $L, \bar{L}$ dyonic fugacities through chiral fermionic bilinears that upset the $\mathrm{U}_A(1)$ symmetry. By a series of bosonic and fermionic techniques, we have explicitly mapped the interacting dyon-antidyon Coulomb liquid with light quarks on a three-dimensional effective theory with fermions. The translationally and parity-invariant ground state was shown to follow from pertinent gap equations. The ground state breaks spontaneously chiral symmetry by developing a fermion condensate. For $N_f = 1$ it does not produce a Goldstone mode because of the $\mathrm{U}_A(1)$ anomaly. We have derived explicit expressions and estimates for masses of the σ and η mesons.

We have shown how the model generalizes to an arbitrary number of flavors and colors. In the whole temperature interval in which our approach is applicable, the ensemble is center symmetric (confining) and breaks spontaneously chiral symmetry provided $x = N_f/N_c < x_\chi \approx 2$. The loss of center symmetry and chiral symmetry restoration in this model seems to occur simultaneously for $x \geq 2$. We have noted that in the case of a very large N_f the fermion-induced interactions maybe too strong to trust the mean-field approximation we used. This point needs to be pursued numerically on the lattice.

This conclusion can be compared to the critical value of $x_\chi \approx 5/3$ of the numerical simulation of the instanton liquid model [14] (first reference). The first simulation of the dyon ensemble with fermions, for $N_c = 2$ [18], found the border line case is $N_f = 4$, also in agreement with $x_\chi \approx 2$. So whether the transition is an artifact of the mean-field approximation or not remains to be studied.

The chiral transition should not be confused with the transition to conformal—fixed infrared coupling—phase, for which current lattice and holographic results put this transition at a much larger number of flavors $x_{\mathrm{conformal}} \approx 4$, or $N_f = 12$ for $N_c = 3$.

Near and above the chiral transition, the fermionic correlations are strong enough to pair L dyons with $\bar{L}$ antidyons into molecules. The dilute regime involved has been explored numerically in [15]. In this paper we only produced some estimates of the transition parameters.

In our approach the confining and chirally broken phases have been treated via the mean-field approximation only, so the resulting gap equation has either a finite or zero Σ, with a finite jump. In the future one can probably include the $L\bar{L}$ correlations in the ensemble. The result would be a depletion of the chiral condensate with perhaps a more continuous cross-over transition as currently observed in QCD-like theories with several flavors of massive quarks.

In the extreme case where all L dyons and $\bar{L}$ antidyons pair to molecules, we have shown that the linearized molecular partition function supports a phase with center symmetry but restored chiral symmetry. It would be interesting in the future to see if such a phase may exist at some N_c, N_f. At this moment, lattice data on that issue are also not clear (see e.g. [25]).

An estimate of the pressure in the center symmetric phase shows that both the free gluon and fermion loop nearly cancel out in leading order in N_c. We have used it to estimate the transition density from a center symmetric phase to a phase with broken center symmetry. A similar estimate of the transition density was made in [1] in the absence of fermions.

The current model can be expanded and improved in a number of ways. The current analysis has been done for the sector with zero θ. As indicated earlier, the L zero modes were selected over the M zero modes, creating a topological unbalance and a lack of manifest θ periodicity in the induced effective action. This can be generalized to an arbitrary θ angle through an extended formalism.

Also, we have not included here some Coulomb corrections discussed in [1], to keep the analysis simpler and to illustrate the interdependence of the center symmetry and the chiral symmetry breaking in this model. These corrections are Debye-like and still within the semiclassical analysis.

Some improvement of the moduli space metric may be considered in the future. We recall that the moduli space metric used in (1) while exact for LM dyons at all separations, is only exact asymptotically for LL, MM dyons. While the former attract, the latter repel. In the center symmetric or confining phase, we expect the like dyons to stay away from each other while the unlike dyons

mingle and screen. In the dyon-antidyon channels, the treatment is so far classical only, with one-loop effects absent. We hope to report on some of these issues, as well as on a full analysis of the meson spectrum for the dyon-antidyon liquid with $N_f > 1$ next.

ACKNOWLEDGMENTS

This work was supported by the U.S. Department of Energy, Office of Science under Contract No. DE-FG-88ER40388.

APPENDIX A: FERMIONIC ZERO MODES AND HOPPING AMPLITUDES

The fermionic zero modes for the L dyon in the hedgehog gauge are defined as $(\varphi_H)^A_\alpha = \eta^A_\beta \epsilon_{\beta\alpha}$ with indices A for color and α for spinors. Their explicit form in terms of $\eta = \eta^+ + \eta^-$ is [15]

$$\eta_{A\alpha} = \frac{\omega_0^{\frac{3}{2}}}{2\sqrt{8\pi}} \frac{\mathrm{th}\frac{\tilde{x}}{2}}{\sqrt{\tilde{x}\mathrm{sh}\tilde{x}}} \times \left((1-\sigma\cdot\hat{r})_{A\alpha} e^{+i\omega_0 x_4} + (1+\sigma\cdot\hat{r})_{A\alpha} e^{-i\omega_0 x_4}\right) \quad \text{(A1)}$$

with $\tilde{x} = \omega_0 r$. For the $\bar{L}$ dyons we have $\pm \to \mp$. Since $\mathrm{Tr}(\varphi_1^\dagger \varphi_2) = \mathrm{Tr}(\eta_1^\dagger \eta_2)$, we may substitute (A1) into (8).

We recall that the "hedgehog" gauge sets the Higgs VEV at large distances to be in the radial direction $\hat{r}$. In this gauge the expressions for the dyon solutions take the simplest and nonsingular form. Unfortunately, for configurations with more than one dyon, one can no longer use this gauge since the "radial direction" cannot be defined. Therefore, it is mandatory to "comb" the dyons into another gauge, in which the direction of the Higgs VEV at large distances is some (arbitrary) constant vector. Such gauges are known as "string" gauges, because the combing produces singularities, the famed Dirac strings.

The "hopping amplitudes" T_{ij} are defined via the Dirac operator, which is by itself gauge invariant, and independent of the particular choice of the gauge. However the "combing rotations" for each dyon depend on the angular coordinates associated with the location of its center, where the Dirac string ends. They are not a global gauge choice, and so they produce some *relative phase factors*, or finite Dirac strings.

Ignoring first the singular combing factor, we readily get the Fourier transform of the hopping matrix. The result is

$$\mathbf{T}(p) = \frac{\omega_0}{2}\left(|A_1(p)|^2 + |A_0'(p)|^2\right), \quad \text{(A2)}$$

with

$$A_n(p) = \frac{\sqrt{2\pi}}{\omega_0^{n+\frac{1}{2}}} \int_0^\infty dx x^{n+\frac{1}{2}} \frac{\sin(\tilde{p}x)}{\tilde{p}x} \frac{\mathrm{th}\frac{x}{2}}{\sqrt{\mathrm{sh}x}}, \quad \text{(A3)}$$

with $\tilde{p} = p/\omega_0$. The two integrals in (A3) for $n = 0, 1$ are carried numerically. All results in the text are derived using (A3).

Now we return to the relative combing factors and show that, in spite of its complicated and singular form, the amendments due to them are small. For that we transform the L zero modes in hedgehog (H) gauge (A1) to the string (S) gauge through a unitary transformation $\varphi_S = U(\theta,\phi)\varphi_H$. Specifically,

$$\varphi_{S,L} = \begin{pmatrix} -\sin\frac{\theta}{2} e^{-i\phi} & +\cos\frac{\theta}{2} \\ -\cos\frac{\theta}{2} & -\sin\frac{\theta}{2} e^{+i\phi} \end{pmatrix} \begin{pmatrix} e^{-i\omega_0 x_4} f(r) \\ e^{+i\omega_0 x_4} f(r) \end{pmatrix}, \quad \text{(A4)}$$

and similarly for the $\bar{L}$ dyon,

$$\varphi_{S,\bar{L}} = \begin{pmatrix} -\cos\frac{\theta}{2} & -\sin\frac{\theta}{2} e^{+i\phi} \\ -\sin\frac{\theta}{2} e^{-i\phi} & +\cos\frac{\theta}{2} \end{pmatrix} \begin{pmatrix} e^{-i\omega_0 x_4} f(r) \\ e^{+i\omega_0 x_4} f(r) \end{pmatrix}, \quad \text{(A5)}$$

with

$$f(r) = \frac{\omega_0^{\frac{3}{2}}}{2\sqrt{8\pi}} \frac{\mathrm{th}\frac{\tilde{x}}{2}}{\sqrt{\tilde{x}\mathrm{sh}\tilde{x}}}. \quad \text{(A6)}$$

The hopping matrix element (8) follows by inserting (A4)–(A5). The integral over the three-dimensional observation point z involves the unitary transformations $U^\dagger(\theta_{x-z}, \phi_{x-z})$ and $U(\theta_{y-z}, \phi_{y-z})$ where the spherical angles θ_{x-z} and θ_{y-z} relative to the Z axis are displayed in Fig. 6, along with the fixed spherical angle $\theta \equiv \theta_{x-y}$.

In general, the hopping matrix element depends nontrivially on the relative angles relative to the Z axis.

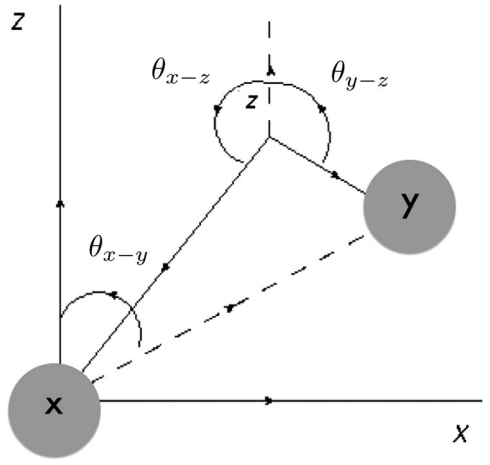

FIG. 6. The grey spheres indicate two dyons centered at **x** and **y**, where z is the observation point. The angles used in the evaluation of the hopping matrix in string gauge are explained. See text.

The following consideration, however, simplify the situation. Since the zero modes decay exponentially, the dominant contribution to the integral in (8) stems from those z with the smallest $|x-z|+|y-z|$, and those are on the line segment connecting x to y. On that segment $\theta_{x-z}=\pi-\theta, \theta_{y-z}=\theta$ and $\phi_{x-z}=\pi, \phi_{y-z}=0$. Most importantly, it can be viewed as only a function of θ which is a constant in the integral. With this in mind, (8) in string gauge reads

$$\mathbf{T}(x-y)\approx +2\omega_0\int d^3z f(|x-z|)f(|y-z|) - 2\left(1+\frac{\cos^2\theta-\cos\theta}{2}\right)\times\int d^3z f|x-z|\frac{f'|y-z|+f|y-z|}{|y-z|}. \quad \text{(A7)}$$

In a large ensemble, we have, on average, $\langle\cos\theta\rangle=0$ and $\langle\cos^2\theta\rangle=\frac{1}{2}$. Thus,

$$\mathbf{T}(x-y)\approx 2\omega_0\int d^3z f(|x-z|)f(|y-z|) - \frac{5}{2}\int d^3z f|x-z|\frac{|y-z|f'|y-z|+f|y-z|}{|y-z|} \quad \text{(A8)}$$

or in Fourier space,

$$\mathbf{T}(p)\approx\frac{\omega_0}{2}\left(|A_1(p)|^2-\frac{5}{4}A_1(p)A_2(p)\right) \quad \text{(A9)}$$

with

$$A_1(p)=\frac{\sqrt{2\pi}}{\tilde{p}\omega_0^{\frac{3}{2}}}\int_0^\infty dx x\sin(\tilde{p}x)\frac{\mathrm{th}\frac{x}{2}}{\sqrt{x\mathrm{sh}x}}$$
$$A_2(p)=\frac{\sqrt{2\pi}}{\tilde{p}\omega_0^{\frac{3}{2}}}\int_0^\infty dx x\sin(\tilde{p}x)\frac{1}{x}\frac{d}{dx}\frac{x\mathrm{th}\frac{x}{2}}{\sqrt{x\mathrm{sh}x}}, \quad \text{(A10)}$$

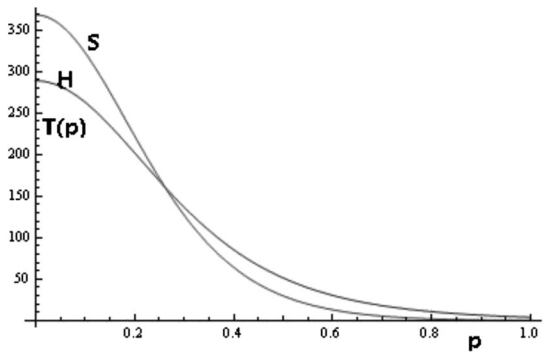

FIG. 7. Hopping matrix $\mathbf{T}(p)$ versus $\tilde{p}$ in hedgehog gauge (A2) (H) and string gauge (A9) (S).

which is to be compared to (A2). The dominant contributions in (A2) and (A9) are due to $|A_1|^2$ which is common to both. In Fig. 7 we compare the hopping in the hedgehog gauge (A2) (H) to that in the string gauge (A9) (S) versus $\tilde{p}$. As expected, the differences are small.

APPENDIX B: ALTERNATIVE FERMIONIZATION

An alternative but equivalent fermionization of the determinant in (13) can be achieved through the use of physical fermionic fields as in [22]. The result is

$$S_f=-i\int d^4x\psi^\dagger\gamma\cdot\partial\psi - i\int d^3x(4\pi f_L v_L e^{w_L-w_M}\theta^+ + 4\pi f_{\tilde{L}} v_l e^{w_{\tilde{L}}-w_{\tilde{M}}}\theta^-), \quad \text{(B1)}$$

with

$$\theta^\pm(z)=\int d^3x\psi^\dagger(x)S_0^{-1}\phi^\pm(x-z)\times\int d^3y\phi^\pm(y-z)S_0^{-1}\psi(y). \quad \text{(B2)}$$

Here $S_0=1/(i\gamma\cdot\partial)$. We have checked that (B1) yields the same partition function after integration as the one we have presented. This can be verified by expanding $\mathrm{Tr}\ln(1+\cdots)$ for the fermionic determinant in each case and carrying the Grassman integration. The advantage in the use of (B1) is in the construction of correlators using operators with the physical fermionic fields.

APPENDIX C: MESON SPECTRUM FOR ARBITRARY N_f

The mesonic spectrum for arbitrary values of N_f can be analyzed using the same reasoning as $N_f=1$. For that we need to modify the Lagrange multipliers through the substitution

$$\lambda(\psi^\dagger\gamma_\pm\psi+\Sigma)\to\sum_{fg}\lambda^\pm_{gf}(\psi^\dagger_f\gamma_\pm\psi_g+\Sigma^\pm_{fg}). \quad \text{(C1)}$$

The multipliers $\lambda_\pm$ are $\mathrm{U(N}_f)\times\mathrm{U(N}_f)$ valued,

$$\lambda_\pm=\lambda_0 e^{\pm i\pi_{ps}/2}(1+\pi_s)e^{\pm i\pi_{ps}/2}, \quad \text{(C2)}$$

with $\pi_{s,ps}=\pi^a_{s,ps}T^a$ and $\mathrm{Tr}(T^aT^b)=\delta^{ab}$ for the $\mathrm{SU(N}_f)$ generators. A rerun of our preceding arguments yield the quadratic actions for $\mathrm{SU(N}_f)\times\mathrm{SU(N}_f)$ pseudoscalar and scalar mesonic actions,

$$S(\pi_{ps,a}) = \frac{1}{2f_\pi^2}\int \frac{d^3p}{(2\pi)^3}\pi_{ps,a}(p)\Delta_-(p)\pi_{ps,a}(p)$$
$$S(\pi_{s,a}) = \frac{1}{2f_\pi^2}\int \frac{d^3p}{(2\pi)^3}\pi_{s,a}(p)\Delta_+(p)\pi_{s,a}(p), \quad \text{(C3)}$$

with

$$\Delta_\mp(p) = 2m\lambda + \int \frac{d^3q}{(2\pi)^3}\frac{(k_1M_2 \mp k_2M_1)}{(k_1^2+M_1^2)(k_2^2+M_2^2)}. \quad \text{(C4)}$$

For the singlets scalar and pseudoscalar $\sigma = \pi_{s,0}$ and $\eta = \pi_{ps,0}$, respectively, we have

$$N_f\Delta_\sigma(p) = \left(\frac{n_D}{N_c} + 2m\lambda\right)\frac{x}{1-x} + \Delta_+(p)$$
$$N_f\Delta_\eta(p) = \left(\frac{n_D}{N_c} + 2m\lambda\right)\frac{x}{1-x} + \Delta_-(p). \quad \text{(C5)}$$

[1] Y. Liu, E. Shuryak, and I. Zahed, Phys. Rev. D **92**, 085006 (2015).
[2] T. C. Kraan and P. van Baal, Nucl. Phys. **B533**, 627 (1998); Phys. Lett. B **435**, 389 (1998); K. M. Lee and C. h. Lu, Phys. Rev. D **58**, 025011 (1998).
[3] D. Diakonov and V. Petrov, Phys. Rev. D **76**, 056001 (2007); **76**, 056001 (2007); AIP Conf. Proc. **1343**, 69 (2011); D. Diakonov, arXiv:1012.2296.
[4] E. Shuryak and T. Sulejmanpasic, Phys. Lett. B **726**, 257 (2013).
[5] R. Larsen and E. Shuryak, arXiv:1408.6563.
[6] D. Diakonov, N. Gromov, V. Petrov, and S. Slizovskiy, Phys. Rev. D **70**, 036003 (2004).
[7] V. A. Fateev, I. V. Frolov, and A. S. Shvarts, Nucl. Phys. **B154**, 1 (1979); B. Berg and M. Luscher, Commun. Math. Phys. **69**, 57 (1979).
[8] A. R. Zhitnitsky, arXiv:hep-ph/0601057; S. Jaimungal and A. R. Zhitnitsky, arXiv:hep-ph/9905540; A. Parnachev and A. R. Zhitnitsky, Phys. Rev. D **78**, 125002 (2008); A. R. Zhitnitsky, Nucl. Phys. **A921**, 1 (2014).
[9] M. Unsal and L. G. Yaffe, Phys. Rev. D **78**, 065035 (2008); M. Unsal, Phys. Rev. D **80**, 065001 (2009).
[10] T. H. Hansson, H. B. Nielsen, and I. Zahed, Nucl. Phys. **B451**, 162 (1995).
[11] E. Poppitz, T. Schfer, and M. Unsal, J. High Energy Phys. 10 (2012) 115; E. Poppitz and M. Unsal, J. High Energy Phys. 07 (2011) 082.
[12] E. Poppitz, T. Schfer, and M. Unsal, J. High Energy Phys. 03 (2013) 087.
[13] D. J. Gross, R. D. Pisarski, and L. G. Yaffe, Rev. Mod. Phys. **53**, 43 (1981); N. Weiss, Phys. Rev. D **25**, 2667 (1982).
[14] T. Schafer and E. V. Shuryak, Rev. Mod. Phys. **70**, 323 (1998); D. Diakonov, Prog. Part. Nucl. Phys. **51**, 173 (2003); M. A. Nowak, M. Rho, and I. Zahed, *Chiral Nuclear Dynamics* (World Scientific, Singapore, 1996).
[15] E. Shuryak and T. Sulejmanpasic, Phys. Rev. D **86**, 036001 (2012).
[16] E. M. Ilgenfritz and E. V. Shuryak, Phys. Lett. B **325**, 263 (1994).
[17] E. Poppitz and T. Sulejmanpasic, J. High Energy Phys. 09 (2013) 128.
[18] P. Faccioli and E. Shuryak, Phys. Rev. D **87**, 074009 (2013).
[19] E. V. Shuryak and I. Zahed, Phys. Rev. D **70**, 054507 (2004).
[20] M. N. Chernodub, T. C. Kraan, and P. van Baal, Nucl. Phys. B, Proc. Suppl. **83**, 556 (2000).
[21] A. M. Polyakov, Nucl. Phys. **B120**, 429 (1977).
[22] M. Kacir, M. Prakash, and I. Zahed, Acta Phys. Pol. B **30**, 287 (1999).
[23] M. Rho, S. J. Sin, and I. Zahed, Phys. Lett. B **689**, 23 (2010); V. Kaplunovsky and J. Sonnenschein, J. High Energy Phys. 04 (2014) 022; S. Bolognesi and P. Sutcliffe, J. Phys. A **47**, 135401 (2014).
[24] M. P. Lombardo, K. Miura, T. N. da Silva, and E. Pallante, *Proc. Sci.*, LATTICE2014 (2014) 242.
[25] A. Hasenfratz, A. Cheng, G. Petropoulos, and D. Schaich, arXiv:1303.7129.
[26] M. Jarvinen and E. Kiritsis, J. High Energy Phys. 03 (2012) 002; R. Alvares, N. Evans, and K. Y. Kim, Phys. Rev. D **86**, 026008 (2012).